Theor Chem Account (2007) 118:511–517
DOI 10.1007/s00214-007-0368-5

REGULAR ARTICLE

Additive intermolecular potentials from *ab initio* calculations: trends in Rg_2–dihalogen van der Waals trimers

Carmen Diez-Pardos · Alvaro Valdés · Rita Prosmiti · Pablo Villarreal · Gerardo Delgado-Barrio

Received: 15 January 2007 / Accepted: 2 February 2007 / Published online: 28 June 2007

Abstract In the present study, the validity of the pairwise additivity of the interactions, derived from the Rg_2 and Rg-dihalogen CCSD(T) potentials, is investigated by means of *ab initio* electronic structure and quantum-mechanical calculations. The topology of the potential surfaces of three different types of Rg_2–dihalogen vdW complexes is studied and general trends within the Rg_2–dihalogen family are discussed. Calculations of vibrational energies, including all five intermolecular degrees of freedom, are performed on such pairwise-additive potentials. The results are compared with experimental data from high-resolution spectroscopy, and provide further information on the additivity of the intermolecular forces for the He_2-dihalogen trimers.

1 Introduction

The intermolecular forces between atoms and molecules are of great importance in studies of solids, liquids and clusters. Over the last decade, enormous advances have been made in understanding of interaction potentials of small molecules. In particular, high-resolution spectra of van der Waals (vdW) complexes have provide information in order to obtain accurate intermolecular potential energy surfaces (PES) for the interaction of rare-gas atoms with small molecules [1–5]. In parallel, developments in *ab initio* techniques and the increase in computer power allow us to calculate intermolecular potentials [6–9].

Despite the advances made in pair potentials, there remains a major obstacle in using such surfaces for studies of condensed phases. This is the problem of non-additivity: the total interaction energy of a cluster is not just the sum of pairwise interactions, but also includes three-body and higher n-body terms. Unfortunately, so far there are no reliable models for the non-additive forces and this precludes the use of accurate pair potentials in simulations of larger complexes. It is difficult to extract information on the three-body forces: a first prerequisite is that the pair potentials involved should be known very accurately, in order to isolate the effects of non-additive forces. Nowdays, sufficiently accurate pair potentials are available for triatomic vdW molecular systems such as Rg–XY where Rg is He, Ne or Ar atom and X,Y=F,Cl,Br or I. In addition, recently high-resolution LIF spectra have been measured for vdW trimers such as He_nICl and He_nBr_2 with $n = 2$ and 3 [10]. The trimer spectra are very sensitive to details of the interaction potential, so that there is now the possibility for obtaining definitive experimental information on non-additive forces in systems containing molecules.

Some progress has already been made toward this objective. Valdés et al. have used pairwise three-body high quality *ab initio* interaction potentials to represent PESs of larger Rg_nXY complexes [11,12]. In particular, ab initio results have been presented for He_2XY (X,Y=Cl, Br and I) systems indicating that pairwise atom–atom interactions are not able to describe the complex, while a sum of three-body He–XY terms [13,14], plus the He–He interaction, can accurately represent the interaction energies for these clusters [11,12]. Such surfaces are of particular interest in the study of both the solvent properties of superfluid helium [15] and the relaxation dynamics of impurities (e.g., dihalogen

Contribution to the Serafin Fraga Memorial Issue.

C. Diez-Pardos · A. Valdés · R. Prosmiti (✉)
P. Villarreal · G. Delgado-Barrio (✉)
Instituto de Matemáticas y Física Fundamental,
C.S.I.C., Serrano 123, 28006 Madrid, Spain
e-mail: rita@imaff.cfmac.csic.es

G. Delgado-Barrio (✉)
e-mail: gerardo@imaff.cfmac.csic.es

molecules) embedded in He nanodroplets and interpretation of recent experimental data [16,17].

In the present study, the validity of the pairwise additivity of the three-body potentials for the Rg_2XY species is investigated. We review here our previous results on He_2XY, with X, Y=Cl, Br, I, complexes [11,12], as well as recent computations on Ar_2ICl one. Comparison between the three different complexes will allow to evaluate the effect of changing the dihalogen upon the vdW bond, as well as the reduced mass of the complex. By analyzing the topology of the PESs, we were able to rationalize the trends within the Rg_nXY family and relate them to properties of the triatomic complexes.

The plan of this paper is as follows. Section 2 will describe the pairwise potentials used for the representation of the PESs and the methodology for the *ab initio* computations. Trends in topology of Rg_2XY are also discussed in Sect. 2. Section 3 describes the computational method used for calculating the energy levels and results obtained, while Sect. 4 summarizes our conclusions.

2 Coordinate system and PESs

The coordinate system used for Rg_2XY is shown in Fig. 1. The positions of the two rare-gas atoms and the center of mass are described by a set of satellite coordinates: r is the bond length of the XY dihalogen; R_1, R_2 are the intermolecular distances of each rare gas atom from the center of mass of the dihalogen, θ_1 is the angle between the $\mathbf{R_1}$ and $\mathbf{r}$ vectors, while θ_2 is the one between $\mathbf{R_2}$ and $\mathbf{r}$, and γ is the angle between the $\mathbf{R_1}$ and $\mathbf{R_2}$ vectors.

2.1 Pairwise-additive potentials

The functional form for the Rg_2XY potential energy function has the form

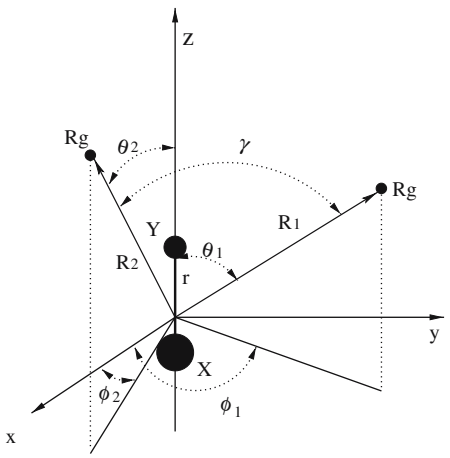

Fig. 1 Coordinate system used for Rg_2XY complexes

$$V(r_e, R_1, R_2, \theta_1, \theta_2, \gamma) = \sum_i V_{\mathrm{Rg}_i XY}(r_e, R_i, \theta_i) + V_{\mathrm{RgRg}}(R_1, R_2, \gamma) \quad (1)$$

The pair potentials used in the present work to construct the above PES follow. (1) The He–He is the potential function for He_2 by Aziz and Slamam [18] fitted to a wide range of experimental data. For Ar–Ar we used a recent *ab initio* CCSD(T) potential function by Slacíĉek et al. [19]. The HFD-B formula has been tested on experimental data such as second virial coefficients, spectral characteristics and scattering data.
(2) The Rg–XY potentials are obtained from [13,14,20]. These surfaces were fitted to high-level CCSD(T) *ab initio* data and their high quality has been also demonstrated by comparisons with experimental measurements from LIF and microwave spectra [21–23]. In comparing calculated quantities with experimental results the quality of the Rg–dihalogen pair potential is crucial. The above triatomic surfaces have proved remarkably successful in predicting the results of experiments. In addition, such potentials have been used successfully to model B ← X excitation spectra [22,24]. Contour plots of different cuts, in XY or ZX Cartesian plane, through the He_2Br_2, He_2ICl and Ar_2ICl surfaces are shown in Fig. 2. The equipotential curves are shown for Rg = He or Ar moving around a triatomic Rg–dihalogen molecule fixed at specific linear (see Fig. 2a) and T-shaped (see Fig. 2b, c) configurations. Contour intervals are of 5 cm^{-1} (left and middle panels) and (a) 25 and (b,c) 50 cm^{-1} (right panel). The energy range is from −80 to −40 cm^{-1} (left panel), −70 to −95 cm^{-1} (middle panel) and −550 to −400 cm^{-1} (right panel) in Fig. 2a, −85 to −40 cm^{-1} (left panel), −55 to −90 cm^{-1} (middle panel) and −550 to −300 cm^{-1} (right panel) in Fig. 2b, and −65 to −40 cm^{-1} (left panel), −45 to −85 cm^{-1} (middle panel) and −550 to −300 cm^{-1} (right panel) in Fig. 2c.

All tetraatomic complexes studied, appear to have different types of minima, namely "police-nightstick", linear, tetrahedral and "bifork" (see Fig. 3). In particular the He_2Br_2 potential has four wells at energies of −97.39, −88.88, −80.38 and 78.04 cm^{-1}, with the collinear well to be the deeper than the "police-nightstick", tetrahedral anf "bifork" ones. For the He_2ICl case the lowest five wells of the potential are found at energies of −97.72, −96.67,−86.38, −85.64 and −77.40 cm^{-1}, for the structures "police-nightstick(1)", linear, "bifork", tetrahedral and "police-nightstick(2)" structures, respectively. The Ar_2ICl surface presents a global minimum at energy −563.76 cm^{-1} for the "police-nightstick(1)" configurations, while local minima are found at energies of −559.39, −556.82, −521.06, −435.47 and −431.07 cm^{-1} for tetrahedral, "bifork", linear, police-nightstick(2) and linear(2) geometries.

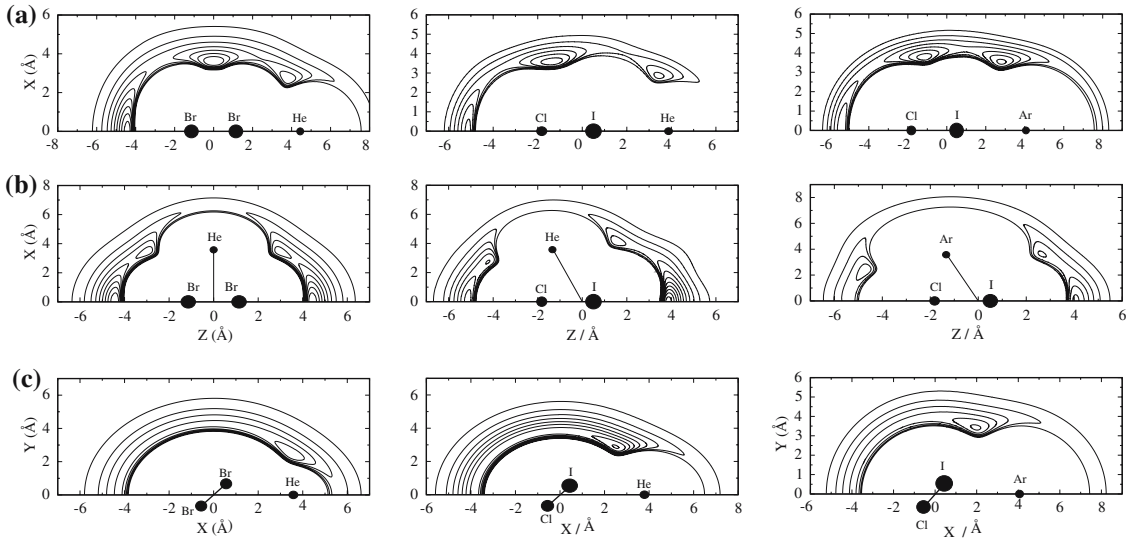

Fig. 2 Contour plots of the potential surfaces (He_2Br_2: *left panel*, He_2ICl: *middle panel* and Ar_2ICl: *right panel*) in the XY (**a**,**b**) or ZX (**c**) plane. The dihalogen bond length distances were kept fixed at their equilibrium values along the *Z* axis, while the geometry of one of the triatomic molecules is fixed to a linear configuration (**a**), or to a near T-shaped configuration (**b** and **c**)

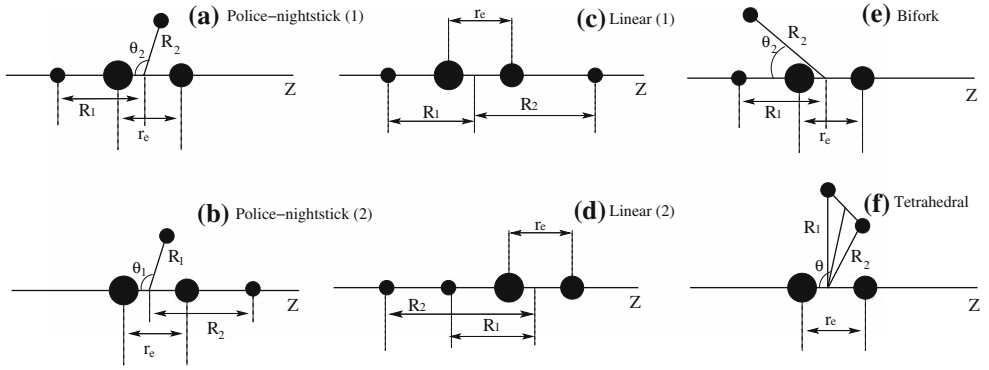

Fig. 3 Configurations of the different types of Rg_2XY Potential minima

2.2 *Ab initio* calculations

Analytical representations based on the sum of three-body He–dihalogen CCSD(T) potentials and He–He interaction (see Eq. 1) have been checked in comparison with the tetraatomic ab initio results. It has been found that such representation of it is able to accurately represent the CCSD(T) tetraatomic data [11,12].

In order to extract information on nonadditive interactions we examine the equilibrium structures based on the above mentioned *ab initio* calculations, by partitioning the interaction energy into components [25]. The *ab initio* calculations were performed using the *Gaussian 98* package [26]. The intermolecular energies were calculated within the supermolecular approach including the correction for the basis-set superposition error. For the heavy halogen atoms (Br and I) we used the Stuttgart–Dresden–Bonn (SDB) large-core energy-consistent pseudopotential [27] in conjunction with the augmented correlation consistent triple zeta (SDB-aug-cc-pVTZ) valence basis set [28]. For the Cl atom we employed the aug-cc-pVTZ basis set while for the He atoms we used the aug-cc-pV5Z from EMSL library [29]. In addition $(3s3p2d2f1g)$ sets of bond functions have been employed in our calculations [14].

In Table 1 we show a summary of supermolecular calculations of the entire nonadditivity in the different HeICl and He_2ICl equilibrium structures using the results of the Møller–Plesset perturbation theory (MPPT) up to fourth order along with the ones of the CCSD(T) method. As can be seen in Table 1, the use of bond functions clearly affects the interaction energies of the complex at the MP2 level, where the second-order dispersion term appears in the analysis of the contents of the two- and three-body supermolecular interaction energies [6]. In turn, the total three-body interaction for different intermolecular configurations around the equilibrium geometries computed through the MP3 amounts

Table 1 Summary of the supermolecular calculations of the nonadditive effects nearby the different equilibrium HeICl and He_2ICl structures

Method	He–ICl system		
	Linear ($\theta = 0$, $R = 3.75$)	T-shaped ($\theta = 112.5$, $R = 3.75$)	Antilinear ($\theta = 180$, $R = 5.0$)
HF	57.83	45.63	54.14
MP2	−50.50	−32.70	−32.04
MP3	−48.59	−32.35	−29.85
MP4(SDQ)	−45.26	−30.31	−26.01
CCSD	−44.18	−29.87	−25.37
CCSD(T)	−56.26	−38.19	−35.45
Method	He_2–ICl system		
	Linear ($R_1 = 3.86$, $R_2 = 5.1$)	Police-nightstick(1) ($R_1 = 3.8$, $R_2 = 3.82$)	Tetrahedral ($R_1 = R_2 = 3.8$)
HF	73.15	79.03	74.25
MP2	−89.52	−88.36	−76.38
MP3	−85.88	−85.97	−76.53
MP4(SDQ)	−79.91	−81.18	−73.04
MP4(SDTQ)	−98.21	−98.63	−87.79
CCSD	−78.53	−79.78	−72.27
CCSD(T)	−97.05	−98.26	−88.32

Energy is in cm^{-1}, angles in degrees and distances in Å

−48.59, −32.35 and −29.85 cm^{-1} for HeICl, while for He_2ICl were −85.88, −85.97 and −76.53 cm^{-1}, respectively. These energies neglect completely the effects of intramonomer correlation on three-body dispersion. The major effect of the intrasystem correlation on dispersion appears in MP4 level and is specially sensitive to the presence of triple excitations. The MP4(SDQ) results seem to be well converged with respect to the CCSD calculations. For a consistent treatment of two and three-body correlation effects, the three-body potentials should be summed to a level of theory one order higher than the one corresponding to the two-body ones. The MP4(SDTQ) reproduces quantitatively the dominant contributions to the two-body interaction energy, while to achieve a similar level of correlation for the three-body terms one needs to turn to next level of theory, CCSD(T) one. Our calculations indicate that the total nonadditive effect in He_2ICl originating from supermolecular CCSD(T) calculations amounts to $0.37, 1.16, -0.53, cm^{-1}$ for configurations nearby the indicated equilibrium structures. As we can see in Table 1 the same behavior is obtained for the MPPT energies for the HeICl complex around its equilibrium configurations.

A similar analysis has also been carried out for $HeBr_2$ and He_2Br_2 complexes, thus it is worthwhile to discuss general trends in the whole set of such complexes. The He_2XY complexes studied appear to have four different types of minima, namely "police-nightstick", linear, tetrahedral and "bifork". The position of their global minimum is opposite and the energy difference between these minima varies for these complexes, but general trends are clearly visible. The relations between various components of intermolecular forces that leads to the ordering of the potential minima are found to be similar between the tetraatomic and triatomic complexes. Thus, we may conclude that for He_2–homopolar dihalogen complexes, the global minimum is expected to be for linear configurations, as all HeX_2 complexes studied appear to have a linear global minimum. In contrast, for heteropolar ones, the location of their global minimum depends on the energy difference balance of the corresponding three triatomic potential wells. Further, the Ar_2ICl case discussed above serves to extent our analysis to heavier members of the Rg_2–dihalogen family. We show that the same types of minima are also presented on its surface. The "police-nightstick" one is the global minimum, while the ordering of the local minima is different than the ones of the He_2ICl complex, with larger energy differences between them. For example, the "bifork" well is deeper than the "linear(1)" one, due to the stronger Ar–Ar interaction compared with the He–He one. However, we should note that the additivity of the three-body ArICl and Ar_2 CCSD(T) interactions for the Ar_2ICl complex, and thus the ordering of its minima, still remains to be checked by *ab initio* computations.

3 Computational method

In order to calculate vibrational levels and structure of the tetraatomic vdW clusters variational quantum treatment was employed. The Hamiltonian used for a Rg_2–dihalogen

trimer is

$$\hat{H} = -\frac{\hbar^2}{2\mu_1}\left(\frac{\partial^2}{\partial R_1^2}+\frac{2}{R_1}\frac{\partial}{\partial R_1}\right)-\frac{\hbar^2}{2\mu_2}\left(\frac{\partial^2}{\partial R_2^2}+\frac{2}{R_2}\frac{\partial}{\partial R_2}\right) + \frac{\hat{j}^2}{2\mu_3 r_e^2}+\frac{\hat{l_1}^2}{2\mu_1 R_1^2}+\frac{\hat{l_2}^2}{2\mu_2 R_2^2}-\frac{\hbar^2}{m_I+m_{Cl}}\nabla_1\cdot\nabla_2 + V(\mathbf{r},\mathbf{R_1},\mathbf{R_2}) \quad (2)$$

where $\mu_1^{-1} = \mu_2^{-1} = m_{\mathrm{Rg}}^{-1} + (m_{\mathrm{X}} + m_{\mathrm{Y}})^{-1}$ and $\mu_3^{-1} = m_{\mathrm{X}}^{-1} + m_{\mathrm{Y}}^{-1}$ are the reduced masses, with m_{Rg}, m_{X} and m_{Y} the atomic masses of He or Ar rare-gas and Br or I and Cl halogen atoms. $\hat{l_1}$, $\hat{l_2}$ and $\hat{j}$ are the angular momenta associated with the vectors $\mathbf{R_1}$ $\mathbf{R_2}$ and $\mathbf{r}$, respectively, leading to a total angular momentum $\hat{J} = \hat{l_1} + \hat{l_2} + \hat{j} = \hat{L} + \hat{j}$. r is fixed at the equilibrium bond length (r_e) for the dihalogen, and the potential for each Rg_2–XY complex is given by the expansion in Eq. (1).

The five dimensional problem for each trimer is solved by diagonalizing the Hamiltonian matrix using a set of basis functions of linear combinations of products of bidimensional radial functions by angular functions:

(a) For the R_1 and R_2 coordinates numerical $\{\xi_n(R_i)\}$, with $i = 1, 2$ and $n = 1, \ldots, N_R$ functions are used.We evaluate them as follows: first, the two-dimensional Schrödinger equation is solved in $(R, \theta; r_e)$ variables for the Rg–XY triatomic system at total angular momentum zero. We employed the corresponding CCSD(T) *ab initio* PES, and a discrete variable representation (DVR) basis set for the R coordinate. It consists of functions given by $f_l(R) = \frac{2}{\sqrt{\mathcal{L}(N+1)}}\sum_{k=1}^{N} \sin\frac{k\pi(R-R^{\min})}{\mathcal{L}} \sin\frac{k\pi l}{N+1}$ where N is the total number of DVR points, $\mathcal{L}$ is $R_i^{\max} - R_i^{\min}$, and the DVR points in the R coordinate are $R^l = \frac{l\mathcal{L}}{N+1} + R^{\min}$ for $l = 1, \ldots, N$. Second, considering a set of the N_R lowest eigenstates, their corresponding radial distributions are orthonormalized through a Gram–Schmidt procedure, and constitute the radial basis set, $\{\xi_n(R_i)\}$, for the tetraatomic calculations.

(b) For the angular basis functions, we consider the following linear combinations, which are eigenfunctions of the parity of total nuclear coordinates inversion p,

$$\mathcal{F}^{(JMp)}_{l_1 l_2 L|\Omega|} = \sqrt{\frac{1}{2(1+\delta_{|\Omega|0})}}\left[\mathcal{W}^{(JM)}_{l_1 l_2 L\Omega} + p(-1)^{J+l_1+l_2+L}\mathcal{W}^{(JM)}_{l_1 l_2 L-\Omega}\right] \quad (3)$$

with

$$\mathcal{W}^{(JM)}_{l_1 l_2 L\Omega} = \sqrt{\frac{2J+1}{4\pi}}\mathcal{D}^{J*}_{M\Omega}(\phi_r, \theta_r, 0)\mathcal{Y}^{L\Omega}_{l_1 l_2}(\mathbf{R_1}, \mathbf{R_2}) \quad (4)$$

M is the projection of J on the space-fixed z axis, Ω its projection on the body-fixed z axis, which is chosen here along the $\mathbf{r}$ vector. The $\mathcal{D}^J_{M\Omega}$ are Wigner matrices [30] and $\mathcal{Y}^{L\Omega}_{l_1 l_2}$ are angular functions in the coupled BF representation.

Taken into account that the Hamiltonian is also invariant under $\mathbf{R_1} \leftrightarrow \mathbf{R_2}$ inversion, then a well-defined parity, p_{12}, basis set is built up as follows:

$$\Phi^{JMpp_{12}}_{l_1 l_2 L|\Omega|nm} = \sqrt{\frac{1}{2(1+\delta_{nm}\delta_{l_1 l_2})}}\left[\Phi^{JMp}_{l_1 l_2 L|\Omega|nm} + p_{12}(-1)^{l_1+l_2+L}\Phi^{JMp}_{l_1 l_2 L|\Omega|mn}\right], \quad (5)$$

where $\Phi^{JMp}_{l_1 l_2 L|\Omega|nm} = \phi_{nm}\mathcal{F}^{(JMp)}_{l_1 l_2 L|\Omega|}$ and $\phi_{nm}(R_1, R_2) = \xi_n(R_1)\xi_m(R_2)/R_1 R_2$.

For the evaluation of the Hamiltonian matrix elements, the numerical set of the radial basis functions $\{\xi_n(R_i)\}$ mentioned above, are represented as linear combinations of the f_l DVR functions, $\xi_n(R_i) = \sum_{l=1}^{N} < \xi_n | f_l > f_l(R_i) = \sum \xi_n(R_i^l) f_l(R_i)$, $i = 1, 2$ and $n = 1, \ldots, N_R$. The full Hamiltonian matrix is constructed in the above basis set as described in [31]. The resulting generalized eigenvalue problem is then solved using routines from the Lapack Library [32,33].

3.1 Results

For the He_2Br_2 and He_2ICl cases we used $N_R = 7$ and 5 radial numerical functions, respectively, represented in both systems at 50 DVR points over the range of 2.5 to 8 Å, for each R_1 and R_2 coordinate. In turn, values of $L = j = 0-12$ (only even in the He2Br2 case) with $l_1^{\max} = l_2^{\max} = 12$ for even ($p_{12} = (-1)^{l_1+l_2+L} = +1$) and $p = (-1)^{J+L+l_1+l_2}$ parity symmetries, were enough to achieve convergence of 0.2 cm^{-1} in the variational calculation, diagonalizing Hamiltonian matrices of order up to $8{,}000 \times 8{,}000$.

For the Ar_2ICl system the angular and radial motion amplitudes are narrower than in the previous cases. This implies the need of larger number of angular functions and fewer radial ones compared with the He_2ICl. Thus, we used $N_R = 3$ radial numerical functions (we choose them as the ground, first and fifth vibrational excited vdW functions of the triatomic) for each $R_{1,2}$ coordinate, represented at 50 DVR over the range of 2.5 to 9 Å, while for the L and $j = 0$–26 values with $l_1^{\max} = l_2^{\max} = 26$ for even p_{12} and p parity symmetries, are used to achieve convergence up to 1 cm^{-1} in the computations for the lower vdW levels. The resulting Hamiltonian matrix is of the order of $24{,}000 \times 24{,}000$ and its diagonalization is computationally more expensive than for the He_2XY systems.

For each trimer the energy levels for the three lowest vibrational states are list in Table 2, while in Fig. 4 the radial $R_{i=1,2}$ and angular $\theta_{i=1,2}$ and γ distributions for these states are shown.

As it can be seen in Fig. 4 for all complexes the lower vibrational wavefunctions are well localized in configuration space. By analyzing them in terms of probability distributions

Table 2 Vibrational energies (in cm^{-1}) for the indicated Rg_2–dihalogen states

Level	Energy/configuration		
	He_2–Br_2	He_2–ICl	Ar_2–ICl
$n = 0$	−32.24/linear	−33.51/police-nightstick(1)	−484.5/police-nightstick(1)
$n = 1$	−31.44/police-nightstick	−31.60/linear	−472.5/police-nightstick(1)
$n = 2$	−30.93/tetrahedral	−30.46/tetrahedral	−469.9/tetrahedral

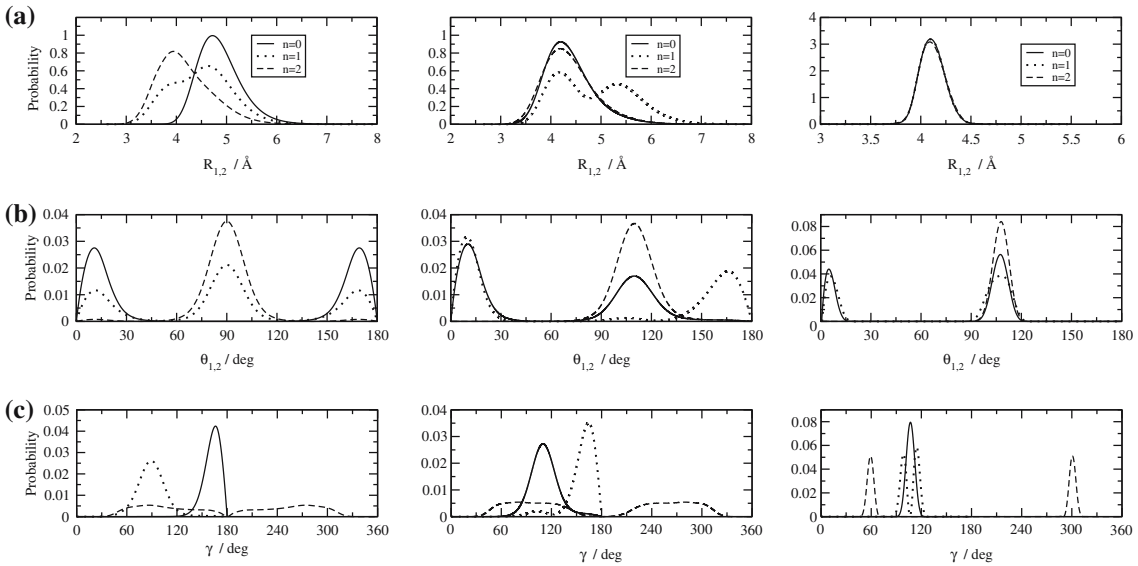

Fig. 4 Radial (**a**) and angular (**b**,**c**) probability densities for the lowest three vibrational vdW levels of He_2Br_2 (*left panel*), He_2ICl (*middle panel*) and Ar_2ICl (*right panel*)

of the internal coordinates the assignment to different conformers could be made. Therefore, vibrationally averaged structures are determined and the dissociation energies these isomers are evaluated. In particular, for He_2Br_2 (see Fig. 4) the $n = 0$ state is localized in the linear well, the $n = 1$ state corresponds to "police-nightstick" configurations, while the $n = 2$ state exhibits a tetrahedral structure. In turn, for He_2ICl (see Fig. 4) a reverse ordering of the two lower states is obtained, with the $n = 0$ state to be localized in the "police-nightstick(1)" well and the $n = 1$ state corresponds to linear configurations. We should note that for both complexes the $n = 2$ distributions present a broad distribution in γ, except small peak at $\gamma \approx 60°$, where the He–He attractive interaction is maximum. In case of Ar_2ICl (see Fig. 4) both $n = 0$ and 1 states are assigned to the "police-nightstick(1)" isomer, while the $n = 2$ to the tetrahedral one. All radial and angular distributions for this complex are very well localized and narrower than the He_2–dihalogen complexes due to the stronger Ar–ICl and Ar–Ar interactions.

For the first two complexes the energy difference between the above mentioned isomers is very small and the lack of the r dependence in the potential form might influence slightly the relative stability. However, recent experimental observations have shown the existence of two different isomers for He_2ICl complex. The "police-nightstick" has been found to be the most strongly bound one, while a second one has been assigned to a distorted tetrahedral structure, with both He atoms in the near T-shaped well [10]. Our CCSD(T) results supports the "police-nightstick(1)" structure as the most stable one in agreement with experimental observations. However, in order to justify the above assertions for such tetraatomic species, further experimental data are needed, and their comparison with our results would finally contribute to evaluate the present surfaces.

4 Conclusions

Three different Rg_2–dihalogen vdW complexes are studied here. The pairwise additivity of the three-body interactions, derived from the Rg_2 and Rg–dihalogen CCSD(T) potentials, is investigated and its validity is checked by means of *ab initio* electronic structure computations for the He_2–dihalogen cases. The intermolecular interactions and structural properties of these clusters, which consist of homopolar and heteropolar halogens, are analyzed and the importance of additional effects, such like introducing electric

dipole moment and larger reduced mass of the complex, is evaluated.

Different structural models, such as "police-nightstick" and "linear", together with the traditional tetrahedral ones based on atom–atom pairwise potentials, are predicted from the above surface calculations. Recent experimental observations have shown the existence of two different isomers for He_2–dihalogen complexes. Unfortunately, no more experimental results are yet available, in order to justify our assertions for the Ar_2ICl case. Further, for the Ar_2–dihalogen system the present results are not yet checked by *ab initio* calculations. It is possible that different contributions to the three-body forces should be considered. Such terms may be arise from the interaction between the permanent multipoles of the hetero-dihalogen molecule and the exchange quadrupole caused by distortion of the two Ar atoms as they overlap. Work in this line is in progress.

Acknowledgments The authors wish to thank the Centro de Calculo de IMAFF, the Centro Técnico de Informática (CTI), CSIC, the Centro de Supercomputación de Galicia (CESGA) and the Grupo de Super-Computación del CIEMAT (GSC) for allocation of computer time. This work has been supported by DGICYT, Spain, Grant No. FIS2004-02461. C.D-P acknowledges C.S.I.C. for the 'Introducción a la investigación' fellowship and R.P. acknowledges support by Ramón y Cajal Programme Grant No. PDRYC-2006-001017.

References

1. Williams J, Rohrbacher A, Seong J, Marianayagam N, Janda KC, Burcl R, Szcześniak MM, Chalasiński G, Cybulski SM, Halberstadt N (1999) J Chem Phys 111:997
2. Higgins K, Tao FM, Klemperer W (1998) J Chem Phys 109:3048
3. Cohen RC, Saykally RJ (1993) J Chem Phys 98:6007
4. Hutson JM (1988) J Chem Phys 89:4550
5. Hutson JM (1992) J Chem Phys 96:6752
6. Chalasinski G, Szczesniak MM (2000) Chem Rev 100:4227
7. Naumkin FY (2001) Chem Phys Chem 2:121
8. Prosmiti R, Cunha C, Villarreal P, Delgado-Barrio G (2003) J Chem Phys 119:4216
9. Prosmiti R, Villarreal P, Delgado-Barrio G (2002) Chem Phys Lett 359:473
10. Loomis RA (private communication)
11. Valdés Á, Prosmiti R, Villarreal P, Delgado-Barrio G (2005) J Chem Phys 122:044305
12. Valdés Á, Prosmiti R, Villarreal P, Delgado-Barrio G (2006) J Chem Phys 125:014313
13. Valdés Á, Prosmiti R, Villarreal P, Delgado-Barrio G (2004) Mol Phys 102:2277
14. Prosmiti R, Cunha C, Villarreal P, Delgado-Barrio G (2002) J Chem Phys 117:7017
15. Draeger EW, Ceperley DM (2003) Phys Rev Lett 90:065301
16. Nauta K, Miller RE (2001) J Chem Phys 115:10138
17. Nauta K, Miller RE (2002) J Chem Phys 117:4846
18. Aziz RA, Slaman MJ (1991) J Chem Phys 94:8047
19. Slavíĉek P, Kalus R, Paŝka P, Odvárková I, Hobza P, Malijevský A (2003) J Chem Phys 119:2102
20. Valdés Á, Prosmiti R, Villarreal P, Delgado-Barrio G (2003) Chem Phys Lett 375:328
21. Boucher DS, Strasfeld DB, Loomis RA, Herbert JM, Ray SE, McCoy AB (2005) J Chem Phys 123:104312
22. McCoy AB, Darr JP, Boucher DS, Winter PR, Bradke MD, Loomis RA (2004) J Chem Phys 120:2677
23. Davey JB, Legon AC, Waclawik ER (1999) Chem Phys Lett 306:133
24. Ray SE, McCoy AB, Glennon JJ, Darr JP, Fesser EJ, Lancaster JR, Loomis RA (2005) J Chem Phys 125:164314
25. Szcześniak MM, Chalasinski G, Piecuch P (1993) J Chem Phys 99:6732
26. Gaussian 98, Revision A.7, Frisch MJ, et al (1998) Gaussian Inc, Pittsburgh PA
27. Bergner A, Dolg M, Kuechle W, Stoll H, Preuss H (1993) Mol Phys 80:1431
28. Martin JML, Sundermann A (2001) J Chem Phys 114:3408
29. Enviromental Molecular Sciences Laboratory, http://www.emsl.pnl.gov/
30. Zare RN (1988) Angular Momentum. Wiley, New York
31. Villarreal P, Roncero O, Delgado-Barrio G (1994) J Chem Phys 101:2217
32. http://www.netlib.org/lapack/
33. http://www.intel.com